



Article (refereed) - postprint

Lucas, Cathy H.; Jones, Daniel O.B.; Hollyhead, Catherine J.; Condon, Robert H.; Duarte, Carlos M.; Graham, William M.; Robinson, Kelly L.; Pitt, Kylie A.; Schildhauer, Mark; Regetz, Jim. 2014 Gelatinous zooplankton biomass in the global oceans: geographic variation and environmental drivers. *Global Ecology and Biogeography*, 23 (7). 701-714.

[10.1111/geb.12169](https://doi.org/10.1111/geb.12169)

Copyright © 2014 John Wiley & Sons, Ltd.

This version available at <http://nora.nerc.ac.uk/507136/>

This is the peer reviewed version of the following article:

Lucas, Cathy H.; Jones, Daniel O.B.; Hollyhead, Catherine J.; Condon, Robert H.; Duarte, Carlos M.; Graham, William M.; Robinson, Kelly L.; Pitt, Kylie A.; Schildhauer, Mark; Regetz, Jim. 2014 Gelatinous zooplankton biomass in the global oceans: geographic variation and environmental drivers. *Global Ecology and Biogeography*, 23 (7). 701-714. [10.1111/geb.12169](https://doi.org/10.1111/geb.12169)

which has been published in final form at <http://dx.doi.org/10.1111/geb.12169>

This article may be used for non-commercial purposes in accordance With Wiley Terms and Conditions for self-archiving.

The definitive version is available at <http://onlinelibrary.wiley.com>

Contact NOC NORA team at
publications@noc.soton.ac.uk

1
2
3
4 1 Gelatinous zooplankton biomass in the global ocean: geographic variation
5
6 2 and environmental drivers
7
8 3
9
10 4

11 5 Cathy H. Lucas^{1,#}, Daniel O. B. Jones¹, Catherine J. Hollyhead^{1,2}, Robert H.
12 6 Condon³, Carlos M. Duarte^{4,5,6}, William M. Graham⁷, Kelly L. Robinson⁷, Kylie
13 7 A. Pitt⁸, Mark Schildhauer⁹, Jim Regetz⁹
14
15
16
17
18
19

20
21 1 National Oceanography Centre, University of Southampton Waterfront Campus, European
22 11 Way, Southampton, SO14 3ZH, UK
23

24 12 cathy.lucas@noc.soton.ac.uk

25 13 dj1@noc.ac.uk
26
27
28

29 15 ²Civil, Maritime and Environmental Engineering and Science Unit, University of
30 16 Southampton, Highfield, Southampton SO17 1BJ, UK.

31 17 cjh1g08@soton.ac.uk
32
33
34

35 19 ³University of North Carolina Wilmington, Department of Biology and Marine Biology, 601
36 20 S. College Road, Wilmington NC, 28403, USA.

37 21 condonr@uncw.edu
38
39
40
41

42 23 ⁴Department of Global Change Research, Instituto Mediterráneo de Estudios Avanzados
43 24 IMEDEA (UIB-CSIC), Esporles, Spain.
44
45
46

47 26 ⁵The UWA Oceans Institute, The University of Western Australia, M470, 35 Stirling
48 27 Highway, Crawley WA 6009 Australia.

49 28 carlos.duarte@uwa.edu.au
50
51
52
53

54 30 ⁶Faculty of Marine Sciences, King Abdulaziz University, P. O. Box 80207, Jeddah 21589
55 31 Saudi Arabia
56
57
58
59
60

1
2
3 33 ⁷Department of Marine Science, The University of Southern Mississippi, 1020 Balch Blvd.,
4
5 34 Stennis Space Center, MS 39529, USA.

6
7 35 Monty.Graham@usm.edu

8
9 36 Kelly.L.Robinson@usm.edu

10 37

11 38 ⁸Australian Rivers Institute and Griffith School of Environment, Griffith University,
12
13 39 Gold Coast Campus, QLD 4111, Australia.

14
15 40 k.pitt@griffith.edu.au

16
17 41

18 42 ⁹National Center for Ecological Analysis and Synthesis (NCEAS), 735 State Street, Santa
19
20 43 Barbara, CA 93101, USA.

21
22 44 schild@nceas.ucsb.edu

23
24 45 regetz@nceas.ucsb.edu

25 46

26
27 47

28
29 48

30 49 #Correspondence: Cathy Lucas: National Oceanography Centre, University of Southampton
31
32 50 Waterfront Campus, European Way, Southampton, SO14 3ZH, UK.

33
34 51 cathy.lucas@noc.soton.ac.uk

35
36 52

37
38 53

39
40 54 **Article type:** Research paper

41
42 55

43
44 56 **Keywords:** Cnidaria, Ctenophora, Thaliacea, jellyfish blooms, JEDI, global ocean,
45
46 57 geographic trends, environmental drivers, macroecology.

47
48 58

49
50 59 **Running title:** Global gelatinous biomass

51
52 60

53
54 61 **Abstract word count:** 299; **Text word count:** 5030

55
56
57
58
59
60

1
2
3 **62 ABSTRACT**
4

5 **63 Aim:** Scientific debate regarding future trends, and subsequent ecological, biogeochemical
6
7 **64** and societal impacts, of gelatinous zooplankton (GZ) in a changing ocean is hampered by
8
9
10 **65** lack of a global baseline and understanding of the causes of biogeographic patterns. We
11
12 **66** address this using a new global database of GZ records to test hypotheses relating to
13
14 **67** environmental drivers of biogeographic variation in the multi-decadal baseline of epipelagic
15
16 **68** GZ biomass in the world's oceans.

17
18
19 **69 Location:** Global ocean.

20
21 **70 Methods:** Over 476,000 global GZ data and metadata were assembled from a variety of
22
23 **71** published and unpublished sources. From this, a total of 91,765 quantitative abundance data
24
25 **72** from 1934 to 2011 were converted to carbon biomass using published biometric equations
26
27 **73** and species-specific average sizes. Total GZ, Cnidaria, Ctenophora and Chordata (Thaliacea)
28
29 **74** biomass was mapped into 5° grid cells and environmental drivers of geographic variation
30
31 **75** tested using spatial linear models.

32
33
34 **76 Results:** We present JeDI (Jellyfish Database Initiative), a publically accessible database
35
36 **77** available at <http://jedi.nceas.ucsb.edu>. We show that: (1) GZ are present throughout the
37
38 **78** world's oceans; (2) global geometric mean and standard deviation of total gelatinous biomass
39
40 **79** is $0.53 \pm 16.16 \text{ mg C m}^{-3}$, corresponding to a global biomass of 38.3 Tg C in the mixed layer
41
42 **80** of the ocean; (3) biomass of all gelatinous phyla is greatest in the subtropical and boreal
43
44 **81** Northern Hemisphere; and (4) within the North Atlantic, dissolved oxygen, apparent oxygen
45
46 **82** utilisation and sea surface temperature are the principal drivers of biomass distribution.
47
48

49
50 **83 Main conclusions:** JeDI is a unique global dataset of GZ taxa, which will provide a
51
52 **84** benchmark against which future observations can be compared and shifting baselines
53
54 **85** assessed. The presence of GZ throughout the world's oceans and across the complete global
55
56
57
58
59
60

1
2
3 86 spectra of environmental variables indicates that evolution has delivered a range of species
4
5 87 able to adapt to all available ecological niches.
6
7
8 88

9
10 89 **INTRODUCTION**

11
12 90 Global climate change and anthropogenic activities are changing the ecology and
13
14 91 biogeography of populations inhabiting the world's oceans, with effects likely to be greatest
15
16 92 in the high latitudes of the Northern Hemisphere (IPCC, 2007; Jones *et al.*, in press).
17
18 93 Empirical evidence indicates that such changes will significantly impact marine ecosystems
19
20 94 and associated ecosystem services including fisheries (Cheung *et al.*, 2010). By
21
22 95 understanding the relationships between biodiversity and biomass, and their biotic and abiotic
23
24 96 drivers, we can begin to predict ecosystem response to future scenarios of climate change,
25
26 97 human impact and habitat loss (Cheung *et al.*, 2008; Beaugrand *et al.*, 2010). These
27
28 98 relationships are well-established for terrestrial ecosystems (Hendriks *et al.*, 2006; Robinson
29
30 99 *et al.*, 2011), but there are far fewer such studies in marine ecosystems owing to the extensive
31
32 100 spatiotemporal variability of the oceans and limited availability of robust data for many
33
34 101 marine taxa, particularly for the open ocean, deep sea, and the Southern Hemisphere (but see
35
36 102 Beaugrand *et al.*, 2010; Tittensor *et al.*, 2010). Additionally, spatial patterns and drivers of
37
38 103 biomass are particularly understudied, with fewer established patterns compared with those
39
40 104 for biodiversity. Whereas plant biomass (Hese *et al.*, 2005) and production (Field *et al.*,
41
42 105 1998) can be resolved from remotely-sensed products, allowing for global patterns to be
43
44 106 examined (Huston & Wolverton, 2009), animal biomass is more elusive. On land, global
45
46 107 patterns of animal abundance have been derived to test hypotheses on the allometric scaling
47
48 108 of population energy use (Currie & Fritz, 1993), and the drivers of global biomass patterns
49
50 109 have also been evaluated for microbial and faunal belowground communities (Fierer *et al.*,
51
52 110 2009). Macroecology, life-history theory and food-web ecology were used to predict global
53
54
55
56
57
58
59
60

1
2
3 111 production and biomass of marine animals (Jennings *et al.*, 2008) with highest teleost fish
4
5 112 biomass reported for productive, cooler upwellings and mid-latitude shelf seas. Food
6
7
8 113 availability influences spatial patterns of global zooplankton biomass (Hernández-León &
9
10 114 Ikeda, 2005) and deep-sea benthic biomass (Wei *et al.*, 2010), and bathymetric changes in the
11
12 115 biomass of deep-sea benthos have also been characterized at the global scale (Rex *et al.*,
13
14 116 2006). In the more physically-complex and variable sedimentary and rocky intertidal habitats,
15
16 117 grain size and wave exposure, respectively are the best predictors of macroinvertebrate
17
18 118 biomass (Ricciardi & Bourget, 1999).
19
20 119
21
22
23 120 Marine zooplankton are crucial for ecosystem function and biogeochemical cycling, linking
24
25 121 primary production to higher trophic levels and deep sea communities, and acting as
26
27 122 hydroclimatic indicators (Richardson, 2008). Gelatinous taxa within the Cnidaria,
28
29 123 Ctenophora, and Chordata (Thaliacea), herein referred collectively as gelatinous zooplankton
30
31 124 (GZ), are ubiquitous members of zooplankton communities and important consumers on
32
33 125 basal production, both as grazers of phytoplankton (thaliaceans) and predators of
34
35 126 zooplankton, fish larvae and other GZ (medusae and ctenophores). They can rapidly
36
37 127 reproduce and form blooms under suitable environmental conditions, and have been widely
38
39 128 reported to have negative ecological and socio-economic impacts: reducing commercially-
40
41 129 harvested fish stocks (Pauly *et al.*, 2009), limiting bioavailable carbon to higher trophic levels
42
43 130 and promoting microbially-mediated food webs (Condon *et al.*, 2011), and causing
44
45 131 detrimental economic impacts on aquaculture, tourism and coastal infrastructure (Purcell *et*
46
47 132 *al.*, 2007). Nonetheless, GZ provide a vital food source for critically-endangered charismatic
48
49 133 species such as the Leatherback turtle *Dermochelys coriacea*, and may even influence their
50
51 134 distribution (Houghton *et al.*, 2006). Additionally, post-bloom jelly-falls may accelerate the
52
53
54
55
56
57
58
59
60

1
2
3 135 biological pump and increase carbon sequestration from the upper ocean to the deep sea-floor
4
5 136 (Lebrato *et al.*, 2012).
6
7
8 137

9
10 138 Fossil evidence and evolutionary supposition indicate cnidarians and ctenophores have
11
12 139 existed for over 500 million years during which they have independently adapted to the major
13
14 140 global climate cycles of warming and cooling and changes in oceanic and atmospheric
15
16 141 conditions; in line with paleoecological insights of long-term resilience for terrestrial species
17
18 142 (Moritz & Agudo, 2013). A recent study has reported increases in regional and global
19
20 143 populations of GZ over decadal timescales (Brotz *et al.*, 2012), although Condon *et al.* (2013)
21
22 144 suggest that GZ blooms display predictable periodic or decadal fluctuations rather than a
23
24 145 sustained monotonic increase. Insufficient long-term quantitative datasets and the lack of a
25
26 146 defined global baseline of gelatinous biomass has been a major limitation to substantiate this
27
28 147 concept. Historically, complete estimation of gelatinous biomass has been hindered by
29
30 148 sampling difficulties associated with their extreme fragility, seasonal periodicity, physical
31
32 149 aggregation and blooming tendencies, paucity of samples from the much of the open ocean
33
34 150 and sampling approaches biased toward non-gelatinous taxa. Recent advances have alleviated
35
36 151 some of these problems; hence, a composite of data sources on GZ abundance have become
37
38 152 available from across the ocean, offering an opportunity to examine the global distribution of
39
40 153 biomass for future reference.
41
42
43
44
45

46 154
47
48 155 The aims of this paper are to (1) define global baselines of carbon biomass for the Cnidaria,
49
50 156 Ctenophora, Chordata (Thaliacea) and total GZ (all 3 phyla combined) within the epipelagic
51
52 157 ocean; (2) identify geographic trends in global GZ biomass by latitude and Longhurst
53
54 158 biogeochemical province; and (3) explore the principal underlying oceanic and environmental
55
56 159 drivers of spatial variation in Cnidaria, Ctenophora and Thaliacea mean biomass, with
57
58
59
60

1
2
3 160 predictor variables chosen on the basis of published studies. As temperature and food
4
5 161 availability are considered to be the most important variables structuring marine ecosystems
6
7 162 (Jennings *et al.*, 2008; Richardson, 2008) we specifically test *a priori* the following
8
9 163 hypotheses relating to biogeographic distribution of gelatinous biomass: 1) GZ biomass is
10
11 164 positively correlated with sea surface temperature, and 2) GZ biomass is greater in regions
12
13 165 characterised by high primary production. Through these efforts we attempt to take a step
14
15 166 towards bridging the current gap between the development of global ecology and
16
17 167 biogeography on land and that at sea; a gap that reflects the much lower research effort, about
18
19 168 10%, in the later domain despite the oceans covering 71% of our planet (Hendriks *et al.*,
20
21 169 2006).
22
23
24
25
26

170

171 **METHODS**

172 **The Jellyfish Database Initiative (JeDI)**

173 JeDI is a scientifically-coordinated global jellyfish database housed at the National Center for
174 Ecological Analysis and Synthesis (Santa Barbara, CA), currently holding over 476,000
175 quantitative, categorical, presence-absence and presence only data on GZ spanning the past
176 four centuries (Appendix S1) (see Condon *et al.*, 2012). GZ data are reported to species level,
177 where identified, but phylum, family and order taxonomic information are reported for all
178 records. Other auxiliary metadata, such as physical, environmental and biometric information
179 relating to the GZ metadata, are included with each respective JeDI entry (Appendix S2).
180 JeDI has also been constructed as a future repository of datasets, and metadata and raw data
181 can be accessed and searched at <http://jedi.nceas.ucsb.edu>.
182

182

183 **Treatment of JeDI and environmental data**

1
2
3 184 Quantitative numerical abundance data (no. m⁻³) of all GZ taxa in the upper 200 m, collected
4
5 185 using a number of sampling gears (Appendix S3), were extracted from JeDI between the
6
7 186 years 1934 and 2011. Abundance was converted into biomass (mg C m⁻³) using species,
8
9 187 family or group-specific length-mass or mass-mass linear and logistic regression equations
10
11 188 (Lucas *et al.*, 2011). Average length measurements for each taxon were taken from the
12
13 189 SeaLifeBase database (www.sealifebase.org), with taxonomic verification provided by the
14
15 190 Catalogue of Life (www.catalogueoflife.org). As biometric equations are not available for all
16
17 191 identified gelatinous taxa, conversions were based on family or class-level comparable
18
19 192 lengths, and where the species epithet was not provided, conversions were computed
20
21 193 assuming the organism belonged to the same genus as previously identified in the same
22
23 194 region. Thirty-three regression equations, representing 18 species of Thaliacea, two
24
25 195 Hydrozoa, seven Scyphozoa, one Nuda and five Tentaculata, were used for abundance to
26
27 196 biomass conversion of 122 species of GZ recorded in JeDI (Appendix S4).
28
29
30
31
32 197
33
34 198 Maps illustrating the spatial distribution of Cnidaria, Ctenophora, Chordata and total GZ
35
36 199 biomass in 5° x 5° grid cells were produced using ArcGIS v10 ESRI. The minimum number
37
38 200 of samples yielding statistically-robust results of the abundance of Cnidaria, Ctenophora,
39
40 201 Thaliacea and total GZ biomass in 5° grid cells was determined by a bootstrapping exercise
41
42 202 whereby ten 5° grid cells were chosen randomly from the 20% of regions with the highest
43
44 203 number of observations. One hundred replicate bootstrapping simulations were run per cell
45
46 204 and the number of observations sampled ranged from 1 - 70 at increasing increments of one
47
48 205 without data replacement. Owing to lack of data for the Ctenophora 1 - 20 observations were
49
50 206 evaluated. To determine the minimum sample size required to adequately characterize the
51
52 207 mean biomass for each cell, relative standard errors (RSE) were compared to the
53
54 208 bootstrapping sample size for each bootstrap run (Appendix S5). These comparisons showed
55
56
57
58
59
60

1
2
3 209 that the RSE decreased rapidly to below 50% after which it stabilised. Using an RSE <50%
4
5 210 as the criteria for adequacy and for consistency across all three taxa, the minimum number of
6
7 211 observations per grid cell that yielded robust results, while retaining sufficient data for
8
9 212 statistical analysis, was 20 data points per grid cell. Consequently, in the North Atlantic
10
11 213 (which contains 219 x 5° cells) 47 cells with <20 observations were removed from analysis,
12
13 214 leaving a total of 109 out of 156 x 5° cells with any data. Subsequent analysis used log₁₀
14
15 215 transformed data and geometric means, to avoid the effect of extreme observations on the
16
17 216 error and further stabilise the variance of data within a cell.
18
19
20
21
22

23 218 For each grid cell, calculations of the arithmetic mean, standard deviation, geometric mean,
24
25 219 geometric standard deviation and coefficient of variation (CV) were computed following the
26
27 220 removal of grid cells containing '0' values. CV highlights areas of the global ocean where the
28
29 221 extent of variability with respect to the mean is greatest and may be used as an indicator of
30
31 222 bloom tendencies defined according to Condon *et al.* (2013). The geometric means were
32
33 223 assigned to their appropriate Longhurst province and ocean basin, using the equator as a
34
35 224 north-south divide. As data were highly skewed (Table 1), the arithmetic mean was deemed
36
37 225 to be an unreliable indication of central tendency and all further synthesis was performed on
38
39 226 the geometric mean.
40
41
42
43
44

45 228 Potential drivers of biomass patterns were chosen based on established hypotheses relating to
46
47 229 temperature (sea surface temperature, SST), productivity (primary production, PP;
48
49 230 chlorophyll *a*, euphotic depth, apparent oxygen utilisation, AOU), oxygen stress (dissolved
50
51 231 oxygen, DO), depth and proximity of coastline (bathymetric depth, distance from coast) that
52
53 232 are known to affect biodiversity and biomass in the marine environment (Tittensor *et al.*,
54
55 233 2010) including GZ. Salinity was not considered as many GZ species (particularly
56
57
58
59
60

1
2
3 234 cnidarians), are euryhaline (see Lucas & Dawson, 2014). Furthermore, productivity can be
4
5 235 used as an indirect indicator for nutrient availability, as jellyfish generally obtain inorganic
6
7 236 nutrients through trophic transfer rather than direct assimilation. This approach encompasses
8
9 237 hypotheses about eutrophication causing jellyfish blooms because jellyfish respond to
10
11 238 productivity caused by eutrophication rather than the nutrients per se. Environmental
12
13 239 parameters were obtained from web-based resources as follows: depth from the National
14
15 240 Geophysical Data Centre (NGDC)
16
17 241 (<http://www.ngdc.noaa.gov/mgg/global/relief/ETOPO2/ETOPO2v2-2006/ETOPO2v2g/>),
18
19 242 surface chlorophyll *a* and SST from the Aqua MODIS satellite
20
21 243 (<http://oceancolor.gsfc.nasa.gov/>), DO and AOU, as netCDF files, from NODC's World
22
23 244 Ocean Atlas 2009, then averaged for the upper 200m of the water column
24
25 245 (http://www.nodc.noaa.gov/OC5/WOA09/netcdf_data.html). Euphotic depth data were from
26
27 246 NASA GIOVANNI Ocean Color Radiometry - Water Quality Portal
28
29 247 (http://gdata1.sci.gsfc.nasa.gov/daac-bin/G3/gui.cgi?instance_id=WaterQuality). Primary
30
31 248 production data were annually-integrated PP, averaged for the years 2003-2011, calculated
32
33 249 with the VGPM algorithm (Behrenfeld & Falkowski, 1997) from MODIS data. Distance from
34
35 250 the coast was calculated from a vector coastline file (<http://www.gadm.org/>) using the
36
37 251 Euclidean Distance tool (spatial analyst extension) in ArcGIS v10. A full summary of GZ
38
39 252 biomass, relative contribution of Cnidaria, Ctenophora and Thaliacea to total GZ by
40
41 253 abundance and biomass, and average values of environmental parameters for each Longhurst
42
43 254 province is given in Appendix S6.
44
45
46
47
48
49
50
51

256 **Statistical analyses and modelling of data**

52
53
54 257 When modelling the relationship between environmental predictors and response variables,
55
56 258 spatial autocorrelation violates the assumptions of traditional statistical approaches (Tittensor
57
58
59
60

1
2
3 259 *et al.*, 2010). Spatial autocorrelation extends to the scale of ocean basins. For the Cnidaria,
4
5 260 semivariance increased linearly with distance, at least to a distance (lag) exceeding 5500 km,
6
7 261 suggesting spatial correlation existed at all scales investigated. For the Thaliacea and
8
9 262 Ctenophora a clear sill was reached, where semivariance stopped increasing, and model fits
10
11 263 suggested that this occurred at distances of 6670 and 3970 km respectively. This spatial
12
13 264 autocorrelation results in deflated estimates of variance and corresponding impacts on
14
15 265 inference, among other issues. As a result, variables were modelled and inference conducted
16
17 266 using both generalized-linear models (GLM) and multivariate spatial linear models (SLM).
18
19 267 Models were developed separately for three taxa (Cnidaria, Ctenophora and Thaliacea),
20
21 268 recognising the differing trophic levels and life history characteristics of the groups.
22
23 269 Following preliminary data exploration, a \log_{10} transformation of the response variables was
24
25 270 selected to homogenise variances and normalise data. GLMs resulted in model residuals that
26
27 271 were spatially non-independent for all taxa in global analyses, and therefore SLM were used
28
29 272 for final inference.
30
31
32
33 273
34
35 274 Spatial analysis was performed using an error-spatial autoregressive (SAR) model (Dormann
36
37 275 *et al.*, 2007), which uses maximum-likelihood spatial autoregression. Neighbourhood
38
39 276 thresholds between 500 and 10,000 km were tested at 100 km intervals and the optimal
40
41 277 neighbourhood size for each taxon was selected by minimising the Akaike information
42
43 278 criterion (AIC) for the spatial null model (the model only retaining a spatial autocorrelation
44
45 279 term). Backward stepwise elimination of insignificant parameters was then used to determine
46
47 280 the minimum adequate model. The importance of individual predictors was assessed through
48
49 281 t-tests (GLM) and z-tests (SLM). Models were tested further by separately including
50
51 282 quadratic terms and interactions between terms; these did not significantly decrease the
52
53 283 deviance of the models compared with the simple models so were not explored further.
54
55
56
57
58
59
60

1
2
3 284 Statistical analysis was carried out using the R programming environment and spatial model
4
5 285 analyses were carried out using R package “spdep” (Bivand *et al.*, 2008). Owing to sparse
6
7
8 286 data in some areas of the world, the analysis was carried out for the North Atlantic only, an
9
10 287 area north of a line between Natal, Brazil, and Bolama, Guinea-Bissau, including the
11
12 288 peripheral seas.
13

14 289

16 290 **RESULTS**

18 291 **Global patterns of gelatinous zooplankton biomass**

19 292 Our quantitative dataset ($n = 91,765$, 5° grid cells = 572) covers 33% of the total ocean area;
20
21 293 43% for the Northern Hemisphere and 23% for the Southern Hemisphere (Fig. 1, Table 2).
22
23

24 294 The global median, and geometric mean and geometric standard deviation of total GZ
25
26 295 biomass in the epipelagic ocean for the past 78 years were 0.81 mg C m^{-3} , and 0.53 ± 16.62
27
28 296 mg C m^{-3} (Table 1). Total GZ biomass varies >7 orders of magnitude across the ocean, with
29
30 297 minimum and maximum geometric means of 2×10^{-4} and $2.3 \times 10^3 \text{ mg C m}^{-3}$ recorded within
31
32 298 the Indian South Subtropical Gyre and North Pacific Tropical Gyre provinces, respectively.
33
34

35 299 Within the major ocean basins, the geometric mean ranged from 0.01 in the South Indian
36
37 300 Ocean to 4.07 mg C m^{-3} in the North Pacific Ocean (Table 2). The highest standard deviation,
38
39 301 ± 47.89 , was recorded from the Arctic.
40
41

42 302

43
44
45 303 Our analysis shows that GZ are present across production gradients from eutrophic coastal
46
47 304 areas to oligotrophic oceanic subtropical gyres, and across temperature gradients from polar
48
49 305 to tropical regions. The top 10% of Longhurst provinces had geometric means of biomass >6
50
51 306 mg C m^{-3} : in the Alaska coastal downwelling ($11.12 \text{ mg C m}^{-3}$), the north-western Atlantic
52
53 307 shelf (6.68 mg C m^{-3}) and the subarctic, tropical and subtropical North Pacific ($6.14 - 14.21$
54
55 308 mg C m^{-3}) (Appendix S6). Coastal and polar regions in the Northern Hemisphere generally
56
57
58
59
60

1
2
3 309 exhibited the highest average and maximum total GZ biomass values compared to those of
4
5 310 the open ocean and Southern Hemisphere (Fig. 1). Maximum total GZ biomass was recorded
6
7 311 along the east coast the USA ($202,838 \text{ mg C m}^{-3}$), the central North Pacific ($35,213 \text{ mg C m}^{-3}$)
8
9 312 3), the Mediterranean ($30,344 \text{ mg C m}^{-3}$), the boreal polar region ($18,582 \text{ mg C m}^{-3}$) and the
10
11 313 shelf seas around the British Isles and Norway ($14,262 \text{ mg C m}^{-3}$) (Fig. 1). While some of
12
13 314 these high biomass regions also exhibit high CV particularly around the coasts, indicating the
14
15 315 co-occurrence of high biomass and GZ blooms in space and time, on a global scale geometric
16
17 316 mean of biomass and CV were negatively correlated ($r_s = -0.21, P < 0.05, n = 579$)
18
19 317 suggesting that many low GZ biomass regions can also be highly influenced by occasional
20
21 318 blooms and sporadic patchiness. Lowest GZ biomass of $<0.01 \text{ mg C m}^{-3}$ was in oligotrophic
22
23 319 or iron-limited Southern Hemisphere regions, including Western Australia, Brazil, the
24
25 320 southern subtropical Indian Ocean and the sub-Antarctic.
26
27
28
29
30
31

32 322 When the three taxa are considered separately, the Thaliacea ($n = 24,998$) and Cnidaria ($n =$
33
34 323 $57,663$) are the most widely distributed (Fig. 2), and contributed the most to total GZ biomass
35
36 324 and abundance (Appendix S6). Ctenophores ($n = 8,757$) were sampled primarily from the
37
38 325 North Atlantic and to a lesser extent the tropical and subtropical North Pacific (Fig. 2). The
39
40 326 global geometric mean and geometric standard deviation of biomass for each phylum were
41
42 327 $0.09 \pm 20.53 \text{ mg C m}^{-3}$ (calculated from 505 grid cells) for the Thaliacea, $4.43 \pm 6.89 \text{ mg C}$
43
44 328 m^{-3} (511 grid cells) for the Cnidaria and $1.14 \pm 24.55 \text{ mg C m}^{-3}$ (227 grid cells) for the
45
46 329 Ctenophora.
47
48
49
50
51

52 331 All three taxa displayed similar latitudinal trends in the geometric mean of biomass (Fig. 3).
53
54 332 The minimum occurs around $20 - 30^\circ\text{S}$, then increases with latitude from the equatorial and
55
56 333 northern subtropical regions to a peak at around $50 - 60^\circ\text{N}$. Although data are sparse and
57
58
59
60

1
2
3 334 variable for the high latitudes, polar regions supported higher GZ biomass. Similarly, the low
4
5 335 number of observations for the Southern Hemisphere makes interpretation of biomass trends
6
7 336 south of 30 - 40° difficult to achieve with a high degree of confidence.
8
9

10 337

11 338 **Environmental drivers of Cnidaria, Ctenophora and Thaliacea biomass**

12
13
14 339 The combination of high spatial autocorrelation, low sample number for the Southern
15
16 340 Hemisphere and asymmetry in latitudinal trend between the north and south, may lead to
17
18 341 misrepresentation of global patterns. As a result, statistical analyses of environmental drivers
19
20 342 for biomass distributions were limited to the North Atlantic where more data are available.
21
22 343 Once spatial autocorrelation had been accounted for, significant relationships with Cnidaria,
23
24 344 Ctenophora and Thaliacea biomass only existed with DO and AOU. SST ($P < 0.05$) was a
25
26 345 significant explanatory variable for biomass of both Thaliacea and Cnidaria. PP ($P < 0.05$)
27
28 346 and distance from coast ($P < 0.05$) were specifically related to only Ctenophora and Cnidaria
29
30 347 biomass distribution respectively. Cnidarians, ctenophores and thaliaceans were found in a
31
32 348 broad range of DO concentrations from 2-8 ml O₂ L⁻¹, with significant linear trends for all
33
34 349 three taxa (Fig. 4 and 5). Significant relationships occurred between AOU and biomass for all
35
36 350 three GZ groups ($P < 0.05$) (Table 3). The partial residual plots showed that these
37
38 351 relationships, once the other environmental variables had been held constant, were positive
39
40 352 for all taxa (Fig. 5). All three GZ taxa were present across the full spectrum of sea surface
41
42 353 temperatures between 0 and 28°C. The linear trends between average biomass and SST were
43
44 354 positive for the Thaliacea ($P < 0.05$) and the Cnidaria ($P < 0.001$), but not significant for the
45
46 355 Ctenophora (Fig. 5, Table 3). There was a significant positive relationship between biomass
47
48 356 of the Ctenophora and PP ($P < 0.05$) (Fig. 5). Cnidaria biomass also increased with
49
50 357 decreasing distance from the coast. There were no significant relationships between biomass
51
52 358 and bathymetric depth, euphotic zone depth or chlorophyll *a*.
53
54
55
56
57
58
59
60

359

DISCUSSION**Gelatinous biomass in the global ocean**

Global estimates of macrozooplankton, and in particular GZ biomass, are extremely rare and are typically accompanied by a number of caveats, mainly relating to uneven spatial coverage of available data across the globe, particularly in the Southern Hemisphere. Our biomass data are significantly more variable than that found by Lynam *et al.* (2011) for the Irish Sea where 62 samples were required to reduce RSE to 5%. None of the 5° grid cells in this study had observed data (not bootstrapped) with an RSE as low as 5%, even those with many thousands of observations. This is most likely a result of the variation in sampling methodologies (Appendix S3) and increased spatial extent of our data from a variety of ocean ecosystems. Moriarty *et al.* (2012) reported a median biomass of 0.19 mg C m⁻³ for macrozooplankton >2 mm sampled from 0 - 350m depth, which is almost twice the depth range used in our analysis (median 0.81 mg C m⁻³ in 0 - 200m depth) and therefore includes regions that sustain lower GZ biomass. Direct comparisons with Lilley *et al.* (2011) are difficult, as their data are expressed as g WW 100 m⁻³, and more significantly, our spatial coverage is more widespread and includes a high proportion of data from the open ocean including the Indian Ocean and the mid-ocean regions of the North Atlantic and Pacific Oceans. Only 31% of the datasets in Lilley *et al.* (2011) are oceanic and many of the other datasets are taken from estuaries, lakes and enclosed seas of the Northern Hemisphere (e.g. Jellyfish Lake in Palau, Honjo Lake in Japan) known to contain significant GZ blooms.

380

We calculate that cnidarians, ctenophores and thaliaceans contribute 92.0 %, 5.5% and 2.5% to an estimated total global GZ biomass of 38.3 Tg C in the upper 200m of ocean (estimated from our GZ geomean of 0.53 mg C m⁻³ and assuming global ocean area = 361,900,000 km²).

383

1
2
3 384 Estimates of global-averaged phytoplankton and zooplankton median biomass are 56 mg C
4
5 385 m⁻³ (Boyce *et al.*, 2010, where mg Chl *a* is converted to C using median Chl:C of 0.01
6
7 386 according to Behrenfeld *et al.*, 2005) and 4.18 mg C m⁻³ (Strömberg *et al.*, 2009: Table A1,
8
9 387 where biomass is modelled from primary production and transfer efficiencies), respectively.
10
11 388 These order of magnitude differences between successive trophic levels (phytoplankton to
12
13 389 zooplankton to GZ) are expected assuming classic food web structure and transfer
14
15 390 efficiencies (Strömberg *et al.*, 2009). Based on two (thaliaceans) or three (cnidarians,
16
17 391 ctenophores) trophic levels, 10% trophic transfer efficiency and 30 - 60 Pg C of primary
18
19 392 production available (Watson *et al.*, 2013), we estimate that < 0.01 - 12 % of the mean annual
20
21 393 global primary production is required to support the estimated global GZ biomass reported in
22
23 394 our study.
24
25
26
27
28
29

30 396 Our global maps and analyses highlight the truly global distribution of GZ in the world's
31
32 397 oceans, from the productive coastal regions where biomass is greatest, to the open ocean and
33
34 398 oligotrophic regions. Nevertheless, clear spatial patterns in biomass are evident. While the
35
36 399 observed latitudinal trends in Cnidaria, Ctenophora and Thaliacea biomass are in broad
37
38 400 agreement with that reported for other macrozooplankton (Moriarty *et al.*, 2012) and
39
40 401 crustacean mesozooplankton (see Hernández-León & Ikeda, 2005: Fig. 1; Strömberg *et al.*,
41
42 402 2009: Fig. 2), the differential between the GZ biomass in the Southern and Northern
43
44 403 Hemispheres is unclear. It may result from low spatial coverage of quantitative samples,
45
46 404 particularly in the Southern Ocean where GZ are known to be abundant, but were unavailable
47
48 405 to JEDI. It may reflect zooplankton food availability for GZ predators; Hernández-León &
49
50 406 Ikeda (2005) suggested that higher zooplankton biomass at 10 - 20°N compared with the
51
52 407 minimal biomass at equivalent latitudes south of the equator was attributed to the productive
53
54 408 north-equatorial waters of the Atlantic Ocean. The reduced coastline in the Southern
55
56
57
58
59
60

1
2
3 409 Hemisphere may be significant for scyphozoan and some hydrozoan jellyfish that require
4
5 410 shallow-water hard surfaces for their benthic polyps to inhabit as part of the cnidarian life
6
7 411 cycle. Finally, lower human impact (e.g. eutrophication, fishing pressure, contaminant loads)
8
9 412 on marine ecosystems in the Southern Hemisphere relative to the Northern Hemisphere
10
11 413 (Halpern *et al.*, 2008) may also influence GZ biomass, as suggested by Purcell *et al.* (2007).
12
13
14
15

414

415 **Environmental drivers of gelatinous biomass**

16
17
18 416 Our analyses suggest that the large-scale spatial trends in the baseline distribution of GZ
19
20 417 biomass in the Atlantic are significantly related to several environmental variables,
21
22 418 particularly SST, DO and primary production. Although data are currently limited, these
23
24 419 trends may apply more generally on global scales but interact synergistically with additional
25
26 420 environmental variables (e.g. riverine nutrient inputs) on local and regional scales (Condon *et*
27
28 421 *al.*, 2013).
29
30
31

422

32
33
34 423 In agreement with Lilley *et al.* (2011), we found no significant correlation with chlorophyll *a*,
35
36 424 although there was a significant relationship between Ctenophora biomass and primary
37
38 425 production. The role of primary production in shaping faunal biomass is a common theme
39
40 426 across several taxa and terrestrial and marine ecosystems (Hernández-Leon & Ikeda, 2005;
41
42 427 Jennings *et al.*, 2008; Fierer *et al.*, 2009), and while correlations with PP might be expected
43
44 428 as it reflects rates of carbon fixation by the entire autotrophic community that ultimately
45
46 429 sustains GZ biomass, it was not a particularly important driver of GZ biomass. The result for
47
48 430 chlorophyll *a* is as expected as chlorophyll *a* indicates the net difference between growth and
49
50 431 removal processes such as viral lysis and grazing.
51
52
53

432

1
2
3 433 There was a broad trend of increasing biomass with increasing DO for all GZ taxa, at the
4
5 434 lower end of this scale relatively high GZ biomass was still distributed in regions of
6
7 435 persistent low DO and hypoxia. Furthermore, high ctenophore biomass was associated with
8
9 436 regions of increased AOU, indicating a connection between GZ biomass and increased
10
11 437 community respiration (del Giorgio & Duarte, 2002). These results further indicate that GZ
12
13 438 may be able to persist in regions unavailable to other pelagic organisms, such as fish, which
14
15 439 are intolerant of low DO conditions ($<4 \text{ mg O}_2 \text{ L}^{-1}$). They are also consistent with previous
16
17 440 studies that suggest several coastal bloom-forming and oceanic GZ species, including *Aurelia*
18
19 441 spp., *Chrysaora quinquecirrha*, *Cyanea capillata*, *Mnemiopsis leidyi* and *Pleurobrachia*
20
21 442 *bachei*, tolerate hypoxic (30% air saturation, $<2 \text{ mg O}_2 \text{ L}^{-1}$) and even severely hypoxic (<0.5
22
23 443 $\text{mg O}_2 \text{ L}^{-1}$) conditions (Thuesen *et al.*, 2005). Furthermore, extreme abundances of the
24
25 444 scyphozoan *Crambionella orsini* have been observed within the Oxygen Minimum Zone
26
27 445 ($<0.5 \text{ mg O}_2 \text{ L}^{-1}$) on the upper slopes off the coast of Oman (Billett *et al.*, 2006). Thus, our
28
29 446 findings show a general trend of increasing GZ biomass with increasing DO levels but
30
31 447 evidence that high GZ biomass can occur in areas of very low DO. The mechanisms by
32
33 448 which GZ can persist under these conditions are not clear and warrant further investigation,
34
35 449 but could be related to the unique allometric (e.g. relatively low carbon demand relative to
36
37 450 individual size) and intracellular physiological characteristics (e.g. anaerobic pathways)
38
39 451 associated with adopting a gelatinous body plan (Pitt *et al.*, 2013). GZ have been shown
40
41 452 experimentally to exhibit comparatively low oxygen thresholds for hypoxia-driven mortality
42
43 453 (Vaquer-Sunyer & Duarte, 2008).
44
45
46
47
48
49
50
51

52 455 Our analysis for the North Atlantic revealed a significant positive linear relationship between
53
54 456 Cnidaria and Thaliacea biomass and SST. This agrees with several other studies that suggest
55
56 457 increased cnidarian and thaliacean biomass is associated with warmer SST (e.g. the
57
58
59
60

1
2
3 458 Mediterranean, Kogovšek *et al.*, 2010; the North Atlantic, Gibbons & Richardson, 2009),
4
5 459 although trends are not universal and species- and geographical-range specific differences in
6
7 460 temperature tolerance will drive differences on local and regional scales (see Zhang *et al.*,
8
9 461 2012). In cnidarians, warmer temperatures generally increase rates of asexual reproduction of
10
11 462 the benthic polyp phase of the life cycle (Lucas *et al.*, 2012), which could increase production
12
13 463 of medusae. For thaliaceans, the mechanisms might also be indirectly driven by SST as
14
15 464 generation times and reproductive output are affected by temperature and food availability
16
17 465 (Lucas & Dawson, 2014). In Antarctica higher salp abundances are observed during warmer
18
19 466 years with low sea ice owing to the higher proliferation of small phytoplankton cells versus
20
21 467 diatoms relative to colder years, which likely reflects their ability to efficiently utilise very
22
23 468 small cells <2 µm at high filtration rates (Sutherland *et al.*, 2010). Thaliaceans are also
24
25 469 prevalent in oligotrophic subtropical gyres where small cells contribute greatly to primary
26
27 470 production or have increased in biomass.
28
29
30
31

471

32
33
34 472 The negative relationship of Cnidarian biomass with distance from coast likely reflects their
35
36 473 life history. Members of the Class Scyphozoa (e.g. *Aurelia* spp., *Cyanea* spp., *Chrysaora*
37
38 474 spp.) dominate cnidarian biomass, the majority of which have a metagenic life cycle that
39
40 475 includes a perennial polyp found attached to natural and artificial substrata in shallow coastal
41
42 476 habitats. Owing to the short lifespan of most cnidarian medusae, the abundance of the adult
43
44 477 population depends on the local polyp populations (Lucas *et al.*, 2012).
45
46
47

478

479 **Concluding remarks and future consequences of GZ biomass**

50
51
52 480 The main drivers of ocean-scale spatial distribution of GZ biomass are SST, DO and AOU;
53
54 481 distance from coast and PP are significant drivers only for the Cnidaria and Ctenophora,
55
56 482 respectively. Nonetheless, the presence of gelatinous taxa across the complete spectra of
57
58
59
60

1
2
3 483 oxygen, temperature and productivity values suggest that the independent evolution of the
4
5 484 gelatinous body plan has delivered a range of phyla that are able to adapt to a wide range of
6
7 485 ecological niches, demonstrated by the truly global presence of gelatinous zooplankton.
8
9 486 Many of the locations that sustain high GZ biomass have experienced increases in SST and
10
11 487 reduced DO over the last three decades at rates greater than the global average, which,
12
13 488 together with other climate- and anthropogenic-driven impacts (Halpern *et al.*, 2008), is
14
15 489 expected to continue. Marked shifts in autotrophic assemblages and primary production are
16
17 490 also predicted to change with large-scale global processes (Blanchard *et al.*, 2012). While the
18
19 491 mechanisms are untested, it has been hypothesized that changes in these physical and
20
21 492 chemical factors will affect the ecology and global distribution of GZ favouring their future
22
23 493 proliferation (Purcell *et al.*, 2007).
24
25
26 494
27
28
29 495 Our spatial analysis is an essential first step in the establishment of a truly appropriate and
30
31 496 uniformly consistent parameterisation of gelatinous presence from which future trends can be
32
33 497 assessed and hypotheses tested, particularly those relating multiple regional and global
34
35 498 drivers on GZ biomass. It complements the recent temporal meta-analysis of Condon *et al.*
36
37 499 (2013) in which global GZ populations (particularly cnidarian medusae) were shown to
38
39 500 exhibit oscillations over multi-decadal timescales centred round a baseline. If GZ biomass
40
41 501 does increase in the future, particularly in the Northern Hemisphere, this may influence
42
43 502 zooplankton and phytoplankton abundance and biodiversity, having a knock-on effect on
44
45 503 ecosystem functioning, biogeochemical cycling (Condon *et al.*, 2011; Lebrato *et al.*, 2012)
46
47 504 and fish biomass (Pauly *et al.*, 2009). The continued development of JeDI and a re-analysis
48
49 505 several decades from now will enable science to determine whether GZ biomass and
50
51 506 distribution alters as a result of anthropogenic climate change.
52
53
54
55
56
57
58
59
60

508 **ACKNOWLEDGMENTS**

509 This research was carried out as part of the Global Jellyfish Project sponsored by the National
510 Center for Ecological Analysis and Synthesis (NCEAS). Funding for NCEAS comes from
511 National Science Foundation (NSF) Grant no. DEB-94-21535, from the University of
512 California at Santa Barbara, and from the State of California. We thank Molly Bogeberg for
513 her contribution to the NCEAS Global Jellyfish Project and construction of JeDI. RHC was
514 also supported by NSF Grant no. NSF-OCE 1030149. CJH carried out the data analysis as
515 part of her Master of Research (Ocean Science) project and was supported by the award of a
516 Richard Newitt prize by the University of Southampton. DOBJ was funded for this work as
517 part of the NERC Marine Environmental Mapping Programme (MAREMAP). We would like
518 to thank Derek Tittensor for his help with the analysis.

519

520

521 **REFERENCES**

- 522 1. Beaugrand, G., Edwards, M. & Legendre, L. (2010) Marine biodiversity, ecosystem
523 functioning, and carbon cycles. *Proceedings of the National Academy of Sciences USA*,
524 **107**, 10120-10124.
- 525 2. Behrenfeld, M.J., Falkowski, P.G. (1997) Photosynthetic rates derived from satellite-
526 based chlorophyll concentration. *Limnology and Oceanography*, **42**, 1-20.
- 527 3. Behrenfeld, M.J., Boss, E., Siegel, D.A & Shea, D.M. (2005) Carbon-based ocean
528 productivity and phytoplankton physiology from space. *Global Biogeochemical Cycles*,
529 **19**, GB1006, doi:10.1029/2004GB002299.
- 530 4. Billett, D.S.M., Bett, B.J., Jacobs, C.L., Rouse, I.P. & Wigham, B.D. (2006) Mass
531 deposition of jellyfish in the deep Arabian Sea. *Limnology and Oceanography*, **51**, 2077-
532 2083.

1
2
3
4
5
6
7
8
9
10
11
12
13
14
15
16
17
18
19
20
21
22
23
24
25
26
27
28
29
30
31
32
33
34
35
36
37
38
39
40
41
42
43
44
45
46
47
48
49
50
51
52
53
54
55
56
57
58
59
60

- 1
2
3 533 5. Bivand, R.S., Pebesma, E.J, Gomez-Rubio, V. (2008) Applied spatial data analysis with
4
5 534 R. Springer, New York. 374 pp.
6
7 535 6. Blanchard, J.L., Jennings, S., Holmes, R., Harle, J., Merino, G., Icarus Allen, J., Holt, J.,
8
9 536 Dulvy, N.K. & Barange, M. (2012) Potential consequences of climate change on primary
10
11 537 production and fish production in large marine ecosystems. *Philosophical Transactions of*
12
13 538 *the Royal Society, Series B*, **367**, 2979-2989.
14
15 539 7. Brotz, L., Cheung, W.W.L., Kleisner, K., Pakhomov, E. & Pauly, D. (2012) Increasing
16
17 540 jellyfish populations: trends in Large Marine Ecosystems. *Hydrobiologia*, **690**, 3-20.
18
19 541 8. Cheung, W.W.L., Close, C., Lam, V., Watson, R. & Pauly, D. (2008) Application of
20
21 542 macroecological theory to predict effects of climate change on global fisheries potential.
22
23 543 *Marine Ecology Progress Series*, **365**, 187-197.
24
25 544 9. Cheung, W.W.L., Lam, V.W.Y., Sarmiento, J.L., Kearney, K., Watson, R., Zeller, D. &
26
27 545 Pauly, D. (2010) Large-scale redistribution of maximum fisheries catch potential in the
28
29 546 global ocean under climate change. *Global Change Biology*, **16**, 24-35.
30
31 547 10. Condon, R.H., Steinberg, D.K., del Giorgio, P.A., Bouvier, T.C., Bronk, D.A., Graham,
32
33 548 W.M. & Ducklow, H.W. (2011) Jellyfish blooms result in a major microbial respiratory
34
35 549 sink of carbon in marine systems. *Proceedings of the National Academy of Sciences of the*
36
37 550 *United States of America*, **108**, 10225-10230.
38
39 551 11. Condon, R.H., Graham, W.M., Duarte, C.M., Pitt, K.A., Lucas, C.H., Haddock, S.H.D.,
40
41 552 Sutherland, K.R., Robinson, K.L., Dawson, M.N., Decker, M.B., Mills, C.E., Purcell,
42
43 553 J.E., Malej, A., Mianzan, H., Uye, S.-I., Gelcich, S. & Madin, L.P. (2012) Questioning
44
45 554 the rise of gelatinous zooplankton in the World's oceans. *Bioscience*, **62**, 160-169.
46
47 555 12. Condon, R.H., Duarte, C.M., Pitt, K.A., Robinson, K.L., Lucas, C.H., Sutherland, K.R.,
48
49 556 Mianzan, H.W., Bogeberg, M., Purcell, J.E., Decker, M.B., Uye, S-I., Madin, L.P.,
50
51 557 Brodeur, R.D., Haddock, S.H.D., Malej, A., Parry, G.D., Erikson, E., Quinoñes, J., Acha,
52
53
54
55
56
57
58
59
60

- 1
2
3 558 M., Harvey, M., Arthur, J.M. & Graham, W.M. (2103) Recurrent jellyfish blooms are a
4
5 559 consequence of global oscillations. *Proceedings of the National Academy of Science of*
6
7 560 *the United States of America*, **110**, 1000-1005.
- 8
9
10 561 13. Currie, D.J. & Fritz, J.T. (1993) Global patterns of animal abundance and species energy
11
12 562 use. *Oikos*, **67**, 56-68.
- 13
14 563 14. del Giorgio, P.A. & Duarte, C.M. (2002) Respiration in the open ocean. *Nature*, **420**, 379-
15
16 564 384.
- 17
18
19 565 15. Dormann, C.F., McPherson, J.M., Araujo, M.B., Bivand, R., Bolliger, J., Carl, G., Davies,
20
21 566 R.G., Hirzel, A., Jetz, W., Kissling, W.D., Kuhn, I., Ohlemuller, R., Peres-Neto, P.R.,
22
23 567 Reineking, B., Schroder, B., Schurr, F.M. & Wilson, R. (2007) Methods to account for
24
25 568 spatial autocorrelation in the analysis of species distributional data: a review. *Ecography*,
26
27 569 **30**, 609-628.
- 28
29
30 570 16. Field, C.B., Behrenfeld, M.J., Randerson, J.T. & Falkowski, P. (1998) Primary production
31
32 571 of the biosphere: integrating terrestrial and oceanic components. *Science*, **281**, 237-240.
- 33
34 572 17. Fierer, N., Strickland, M.S., Liptzin, D., Bradford, M.A. & Cleveland, C. (2009) Global
35
36 573 patterns in belowground communities. *Ecology Letters*, **12**, 1238-1249.
- 37
38
39 574 18. Gibbons, M.J. & Richardson, A.J. (2009) Patterns of jellyfish abundance in the North
40
41 575 Atlantic. *Hydrobiologia*, **616**, 51-65.
- 42
43 576 19. Halpern, B.S., Walbridge, S., Selkoe, K.A., Kappel, C.V., Micheli, F., Agrosa, C.D.,
44
45 577 Bruno, J.F., Casey, K.S., Ebert, C., Fox, H.E., Fujita, R., Heinemann, D., Lenihan, H.S.,
46
47 578 Madin, E.M.P, Perry, M.T., Selig, E.R., Spalding, M., Steneck, R. & Watson, R. (2008) A
48
49 579 global map of human impact on marine ecosystems. *Science*, **319**, 948-952.
- 50
51
52 580 20. Hendriks, I.E., Duarte, C.M. & Heip, C.H.R. (2006) Biodiversity research still grounded.
53
54 581 *Science*, **312**, 1715.
- 55
56
57
58
59
60

- 1
2
3 582 21. Hernández-León, S. & Ikeda, T. (2005) A global assessment of mesozooplankton
4
5 583 respiration in the ocean. *Journal of Plankton Research*, **27**, 153-158.
6
7
8 584 22. Hese, S., Lucht, W., Schmullius, C., Barnsley, M., Dubayah, R., Knorr, D., Neumann, K.,
9
10 585 Riedel, T. & Schröter, K. (2005) Global biomass mapping for an improved understanding
11
12 586 of the CO₂ balance – the Earth observation mission Carbon-3D. *Remote Sensing of*
13
14 587 *Environment*, **94**, 94-104.
15
16
17 588 23. Houghton, J.D.R., Doyle, T.K., Wilson, M.W., Davenport, J. & Hays, G.C. (2006)
18
19 589 Jellyfish aggregations and leatherback turtle foraging patterns in a temperate coastal
20
21 590 environment. *Ecology*, **87**, 1967-1972.
22
23 591 24. Huston, M.A. & Wolverton, S. (2009) The global distribution of net primary production:
24
25 592 resolving the paradox. *Ecological Monographs*, **79**, 343-377.
26
27
28 593 25. IPCC (Intergovernmental Panel on Climate Change) (2007) Summary for policymakers.
29
30 594 In: Solomon, S., Qin, D., Manning, M., Chen, Z. *et al.* (eds) Climate change 2007: the
31
32 595 physical science basis. Contribution of Working Group I to the Fourth Assessment Report
33
34 596 of the Intergovernmental Panel on Climate Change. Cambridge University Press, New
35
36 597 York, p 1–18.
37
38
39 598 26. Jennings, S., Mélin, F., Blanchard, J.L., Forster, R.M., Dulvy, N.K. & Wilson, R.W.
40
41 599 (2008) Global-scale predictions of community and ecosystem properties from simple
42
43 600 ecological theory. *Proceedings of the Royal Society B*, **275**, 1375-1383.
44
45
46 601 27. Jones, D.O.B., Yool, A., Wei, C-L., Henson, S.A., Ruhl, H.A., Watson, R.A. & Gehlen,
47
48 602 M. (in press) Global reductions in seafloor biomass in response to climate change. *Global*
49
50 603 *Change Biology*
51
52 604 28. Kogovšek, T., Bogunović, B. & Malej, A. (2010) Recurrence of bloom-forming
53
54 605 scyphomedusae: wavelet analysis of a 200-year time series. *Hydrobiologia*, **645**, 81-96.
55
56
57
58
59
60

- 1
2
3 606 29. Lebrato, M., Pitt, K.A., Sweetman, A.K., Jones, D.O.B., Cartes, J.E., Oschlies, A.,
4
5 607 Condon, R.H., Molinero, J.C., Adler, L., Gaillard, C., Lloris, D. & Billett, D.S.M. (2012)
6
7 608 Jelly-falls historic and recent observations: a review to drive future research directions.
8
9 609 *Hydrobiologia*, **690**, 227-245.
- 10
11
12 610 30. Lilley, M.K.S., Beggs, S.E., Doyle, T.K., Hobson, V.J., Stromberg, K.H.P. & Hays, G.C.
13
14 611 (2011) Global patterns of epipelagic gelatinous zooplankton biomass. *Marine Biology*,
15
16 612 **158**, 2429-2436.
- 17
18
19 613 31. Lucas, C.H. & Dawson, M.N. (2014) What are jellyfishes and thaliaceans and why do
20
21 614 they bloom? In: Pitt, K.A. & Lucas, C.H. (eds) *Jellyfish Blooms*, Springer. pp 9 - 44. doi:
22
23 615 10.1007/978-94-007-7015-7
- 24
25
26 616 32. Lucas, C.H., Pitt, K.A., Purcell, J.E., Lebrato, M. & Condon, R.H. (2011) What's in a
27
28 617 jellyfish? Proximate and elemental composition and biometric relationships for use in
29
30 618 biogeochemical studies. *Ecology*, **92**, 1704.
- 31
32
33 619 33. Lucas, C.H., Graham, W.M. & Widmer, C. (2012) Jellyfish life histories: the role of
34
35 620 polyps in forming and maintaining scyphomedusa populations. *Advances in Marine*
36
37 621 *Biology*, **63**, 33-196.
- 38
39 622 34. Lynam, C.P, Lilley, M.K.S., Bastian, T., Doyle, T.K., Beggs, C.E. & Hays, G.C. (2011)
40
41 623 Have jellyfish in the Irish Sea benefited from climate change and overfishing? *Global*
42
43 624 *Change Biology*, **17**, 767-782.
- 44
45
46 625 35. Moriarty, R., Buitenhuis, E.T., Le Quéré, C. & Gosselin, M.-P. (2012) Distribution of
47
48 626 known macrozooplankton abundance and biomass in the global ocean. *Earth System*
49
50 627 *Science Data Discussions*, **5**, 187-220.
- 51
52
53 628 36. Moritz, C. & Agudo, R. (2013) The future of species under climate change. Resilience or
54
55 629 decline? *Science*, **341**, 504-508.
- 56
57
58
59
60

- 1
2
3 630 37. Pauly, D., Graham, W., Libralato, S., Morissette, L. & Palomares, M.L.D. (2009)
4
5 631 Jellyfish in ecosystems, online databases, and ecosystem models. *Hydrobiologia*, **616**, 67-
6
7 632 85.
8
9
10 633 38. Pitt, K.A., Duarte, C.M., Lucas, C.H., Sutherland, K.R., Condon, R.H., Mianzan, H.,
11
12 634 Purcell, J.E., Robinson, K.R., Uye, S.-I. (2013) Jellyfish body plans provide allometric
13
14 635 advantages beyond low carbon content. *PLoS ONE*, **8(8)**, e72683.
15
16
17 636 39. Purcell, J.E., Uye, S.-I. & Lo, W.-T. (2007) Anthropogenic causes of jellyfish blooms and
18
19 637 their direct consequences for humans: a review. *Marine Ecology Progress Series*, **350**,
20
21 638 153-174.
22
23 639 40. Rex, M.A., Etter, R.J., Morris, J.M., Crouse, J., McClain, C.R., Johnson, N.A., Stuart,
24
25 640 C.T., Deming, J.W., Thies, R. & Avery, R. (2008) Global bathymetric patterns of
26
27 641 standing stock and body size in the deep-sea benthos. *Marine Ecology Progress Series*,
28
29 642 **317**, 1-8.
30
31
32 643 41. Richardson, A.J. (2008) In hot water: zooplankton and climate change. *ICES Journal of*
33
34 644 *Marine Science*, **65**, 279-295.
35
36
37 645 42. Robinson, L.M., Elith, J., Hobday, A.J., Pearson, R.G., Kendall, B.E., Possingham, H.P.
38
39 646 & Richardson, A.J. (2011) Pushing the limits in marine species distribution modelling:
40
41 647 lessons from the land present challenges and opportunities. *Global Ecology and*
42
43 648 *Biogeography*, **20**, 789-802.
44
45
46 649 43. Ricciardi, A. & Bourget, E. (1999) Global patterns of macroinvertebrate biomass in
47
48 650 marine intertidal communities. *Marine Ecology Progress Series*, **185**, 21-35.
49
50 651 44. Strömberg, K.H.P., Smyth, T.J., Allen, J.I., Pitois, S. & O'Brien, T.D. (2009) Estimation
51
52 652 of global zooplankton biomass from satellite ocean colour. *Journal of Marine Systems*,
53
54 653 **78**, 18-27.
55
56
57
58
59
60

- 1
2
3 654 45. Sutherland, K.R., Madin, L.P. & Stocker, R. (2010) Filtration of submicrometer particles
4
5 655 by pelagic tunicates. *Proceedings of the National Academy of Science of the United States*
6
7 656 *of America*, **107**, 15129-15134.
8
9
10 657 46. Thuesen, E.V., Rutherford, L.D., Brommer, P.L., Garrison, K., Gutowska, M.A. &
11
12 658 Towanda, T. (2005) Intragel oxygen promotes hypoxia tolerance of scyphomedusae.
13
14 659 *Journal of Experimental Biology*, **208**, 2475-2482.
15
16
17 660 47. Tittensor, D.T., Mora, C., Jetz, W., Lotze, H.K., Ricard, D., Berghe, E.V. & Worm, B.
18
19 661 (2010) Global patterns and predictors of marine biodiversity across taxa. *Nature*, **466**,
20
21 662 1098-1101.
22
23 663 48. Vaquer-Sunyer, R. & Duarte, C.M. (2008) Thresholds of hypoxia for marine biodiversity.
24
25 664 *Proceedings of the National Academy of Sciences of the United States of America*, **105**,
26
27 665 15452–15457.
28
29
30 666 49. Watson, R., Zeller, D. & Pauly, D. (2013) Primary production demands of global
31
32 667 fisheries. *Fish and Fisheries*, doi: 10.1111/faf.12013.
33
34
35 668 50. Wei, C-L., Rowe, G.T., Escobar-Briones, E., Boetius, A., Soltwedel, T., Caley, M.J.,
36
37 669 Soliman, Y., Huettmann, F., Qu, F., Yu, Z., Pitcher, C.R., Haedrich, R.L., Wicksten,
38
39 670 M.K., Rex, M.A., Baguley, J.G., Sharma, J., Danovaro, R., MacDonald, I.R., Nunnally,
40
41 671 C.C., Deming, J.W., Montagna, P., Lévesque, M., Weslawski, J.M., Wlodarska-
42
43 672 Kowalczuk, M., Ingole, B.S., Bett, B.J., Billett, D.S.M., Yool, A., Bluhm, B.A., Iken, K.
44
45 673 & Narayanaswamy, B.E. (2010) Global patterns and predictions of seafloor biomass
46
47 674 using random forests. *PLoS ONE*, **5(12)**, e15323.
48
49
50 675 51. Zhang, F., Sun, S., Jin, X.S. & Li, C.L. (2012) Associations of large jellyfish distributions
51
52 676 with temperature and salinity in the Yellow Sea and East China Sea. *Hydrobiologia*, **690**,
53
54 677 81-96.
55
56
57 678
58
59
60

679 **BIOSKETCH**

Catherine Hollyhead is currently studying for an EngD at the University of Southampton. Cathy Lucas, Rob Condon, Carlos Duarte, Monty Graham, Kelly Robinson and Kylie Pitt are all members of an NCEAS working group titled “Global expansion of jellyfish blooms: Magnitude, causes and consequences” <http://www.nceas.ucsb.edu/projects/12479>. Mark Schildauer and Jim Regertz are or were based at NCEAS. Daniel Jones is a researcher in deep-sea biology, with a particular interest in the reservoirs and fate of global gelatinous zooplankton biomass. Author contributions: CHL, CJH, RHC and DOBJ wrote the article; CJH, CHL, RHC & CMD designed the study; DOBJ & CJH analysed the data and prepared the figures; WMG, KLR, KAP, CHL & RHC compiled and assembled the datasets in JeDI, MS & JR provided database technical support at NCEAS. All authors commented on drafts of the manuscript and contributed substantially to revisions.

680

SUPPORTING INFORMATION

Appendix S1. Maps of the Jellyfish Database Initiative (JeDI) database.

Appendix S2. Template used to gather data for entry into the Jellyfish Database Initiative (JeDI) database.

Appendix S3. Relative contribution of different sampling methods used to collect quantitative gelatinous zooplankton data.

Appendix S4. Published biometric equations and body composition ratios used to convert gelatinous zooplankton species abundance into carbon biomass.

Appendix S5. Relative standard errors (RSE) in the mean as a function of the number of observations within a 5° grid cell.

Appendix S6. Summary of environmental and gelatinous zooplankton data for each Longhurst province.

TABLES

Table 1. Summary of descriptive statistics of global biomass (mg C m^{-3}) of medusae (phylum Cnidaria), ctenophores (phylum Ctenophora) and pelagic tunicates (phylum Chordata), based upon 5° gridded data comprising 91,765 samples taken from the Jellyfish Database Initiative (JeDI). GZ = gelatinous zooplankton; n = number of observations; Mean = geometric mean for biomass and arithmetic mean for all other variables; SD = standard deviation; P(SWilk) = probability of a normal distribution based on a Kolmogorov-Smirnov test; SST = sea surface temperature; DO = dissolved oxygen; AOU = apparent oxygen utilisation.

Variable	n	Mean \pm SD	Maximum	Median	Skewness	P(SWilk)
Total GZ biomass (mg C m^{-3})	572	0.53 ± 16.62	2292.06	0.81	17.61	<0.001
Bathymetric depth (m)	579	3,121 $\pm 1,921$	6,040	3,778	0.49	<0.001
Chlorophyll <i>a</i> (mg m^{-3})	492	0.57 ± 1.17	8.50	0.19	4.05	<0.001
SST ($^\circ\text{C}$)	492	20.02 ± 9.54	32.08	24.07	-0.98	<0.001
DO (ml L^{-1})	500	4.69 ± 1.30	7.90	4.65	0.29	<0.001
AOU (ml L^{-1})	495	1.32 ± 0.78	4.17	1.06	1.16	<0.001
Euphotic zone depth (m)	575	74.9 ± 28.3	142.4	77.7	-0.03	<0.001
Primary production ($\text{g C m}^{-2} \text{yr}^{-1}$)	575	229.2 ± 235.5	1593.6	154.0	2.80	<0.001
Distance from coast (km)	579	623 ± 621	5,878	465	1.80	<0.001

Table 2. The geometric mean and geometric standard deviation (SD) of total GZ biomass (mg C m^{-3}) for each ocean basin and the Mediterranean Sea (Med). The calculations were performed upon the allocated 5° grid cells from the associated Longhurst province with the equator as the north-south divide. For each ocean basin and sea, the number of 5° grid cells and the percentage cover this represents, for which quantitative data were available and from which the calculations were made is also shown.

	Arctic	North Atlantic	South Atlantic	Med	North Pacific	South Pacific	North Indian	South Indian	Southern
Percentage cover	16%	80%	34%	59%	39%	14%	82%	39%	2%
Number of grid cells	46	140	57	10	129	51	49	94	3
Mean (mg C m^{-3})	1.38	1.61	0.17	0.22	4.07	0.37	0.13	0.01	3.63
SD (mg C m^{-3})	47.98	7.53	6.60	5.48	7.00	8.58	3.11	6.72	1.76

Table 3. Generalized-linear model (GLM) and spatial linear model (SLM) results for minimal adequate models using North Atlantic data. Numbers indicate t-values (GLM) or z-values (SLM), asterisks indicate significance of individual predictors: * $p < 0.05$; ** $p < 0.01$; *** $p < 0.001$ and ns is not significant. Coefficients are presented in parentheses. AIC = Akaike information criterion, SST = sea surface temperature, DO = dissolved oxygen, AOU = apparent oxygen utilisation. Moran's I is calculated on the model residuals.

	Ctenophores		Thaliaceans		Cnidarians	
	GLM	SLM	GLM	SLM	GLM	SLM
Bathymetric depth						
Chlorophyll <i>a</i>						
SST			(0.17)	(0.13)	(0.06)	(0.05)
			5.36***	3.76***	2.22*	2.43*
DO	(0.29)	(0.24)	(1.68)	(1.28)	(0.55)	(0.58)
	3.60***	2.28*	5.64***	3.98***	2.71**	2.82**
AOU	(0.46)	(0.34)	(1.63)	(1.24)	(0.46)	(0.49)
	4.27***	2.70**	5.29***	4.05***	2.09*	2.20*
Euphotic zone depth						
Primary production	(0.001)	(0.001)				
	2.69**	2.71**				
Distance from coast					(-0.001)	(-0.001)
					-2.24*	-2.30*
R ² (GLM) / Pseudo R ² (SLM)	0.27	0.26	0.29	0.19	0.09	0.35
AIC	144.69	143.18	179.94	176.64	103.74	104.86
Moran's I	0.139*	0.016 ns	0.193**	0.022 ns	0.087 ns	0.007 ns

FIGURE LEGENDS

Figure 1. Maps of 5° grid cells data of sampled total gelatinous zooplankton plotted over Longhurst provinces of (a) number of sample observations; (b) maximum biomass (mg C m^{-3}); (c) geometric mean of biomass (mg C m^{-3}); and (d) coefficient of variation using the arithmetic mean of biomass. Areas where there are no observations are indicated by light blue (sea).

Figure 2. Maps of 5° grid cells data of geometric mean biomass (mg C m^{-3}) plotted over Longhurst Provinces of (a) Cnidaria; (b) Ctenophora; and (c) Thaliacea. Areas where there are no observations are indicated by light blue (sea).

Figure 3. Latitudinal trends of global biomass of (a) Cnidaria; (b) Ctenophora; and (c) Thaliacea. Trends indicated by fit from single-variable linear models (lines with grey area indicating 95% confidence limits). Note log (base 10) scale on y axis.

Figure 4. Scatterplots showing significant relationships between biomass of Ctenophora (a-c), Thaliacea (d-f) and Cnidaria (g-j) and environmental variables in the North Atlantic. DO = dissolved oxygen, AOU = apparent oxygen utilisation, SST = sea surface temperature, PP = primary production. Note log (base 10) scale on y axis.

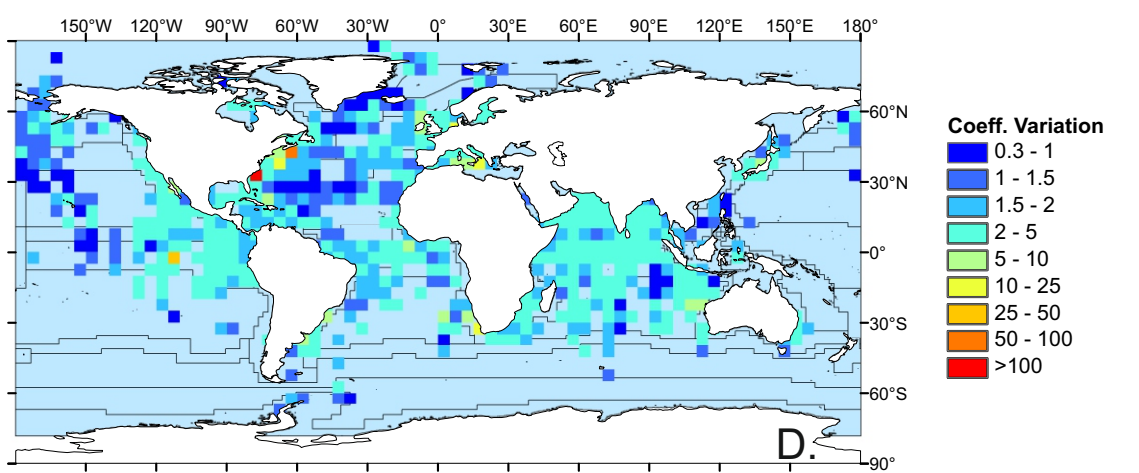
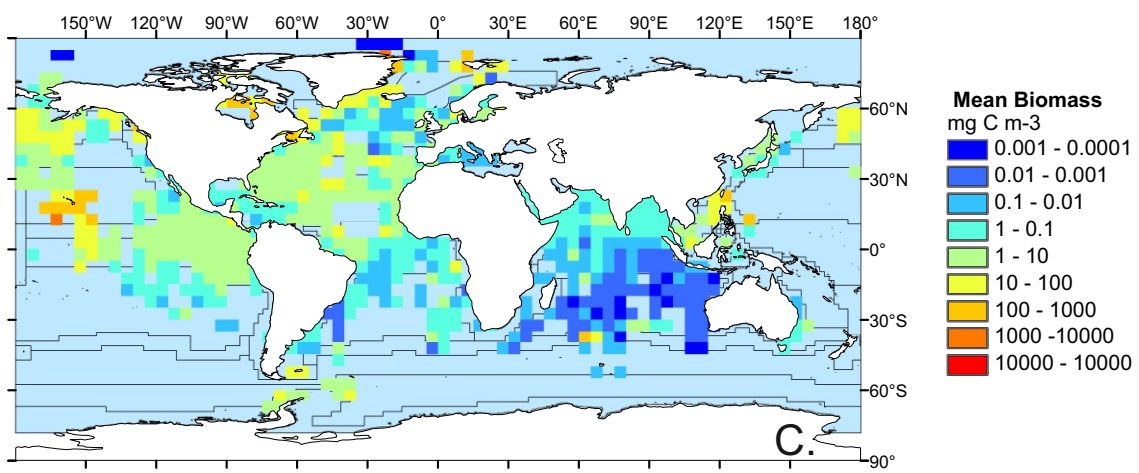
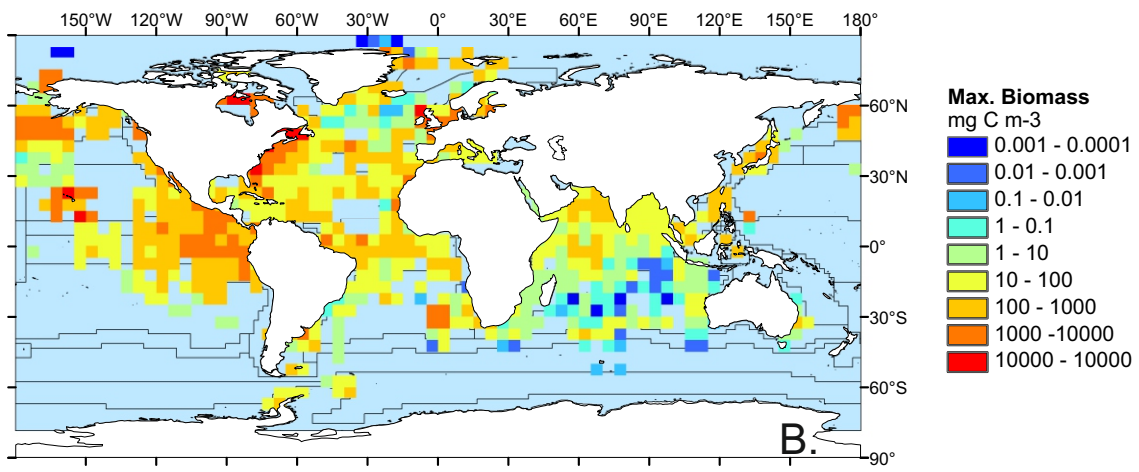
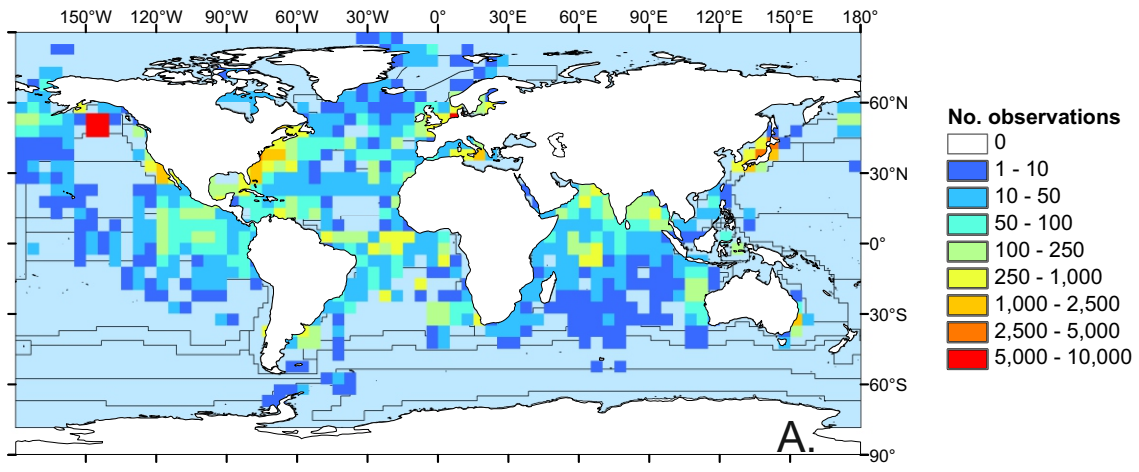
Figure 5. Partial residual plots for the predictors of the minimum adequate SLM biomass of Ctenophora (a-c), Thaliacea (d-f) and Cnidaria (g-j) and environmental variables in the North Atlantic. Plots show the individual effects of: DO = dissolved oxygen, AOU = apparent oxygen utilisation, SST = sea surface temperature, PP = primary production, Euphotic depth = euphotic zone depth. A partial residual plot is a plot of $r_i + b_k^*i_k$ vs. x_{ik} , where r_i is the

1
2
3
4
5
6
7
8
9
10
11
12
13
14
15
16
17
18
19
20
21
22
23
24
25
26
27
28
29
30
31
32
33
34
35
36
37
38
39
40
41
42
43
44
45
46
47
48
49
50
51
52
53
54
55
56
57
58
59
60

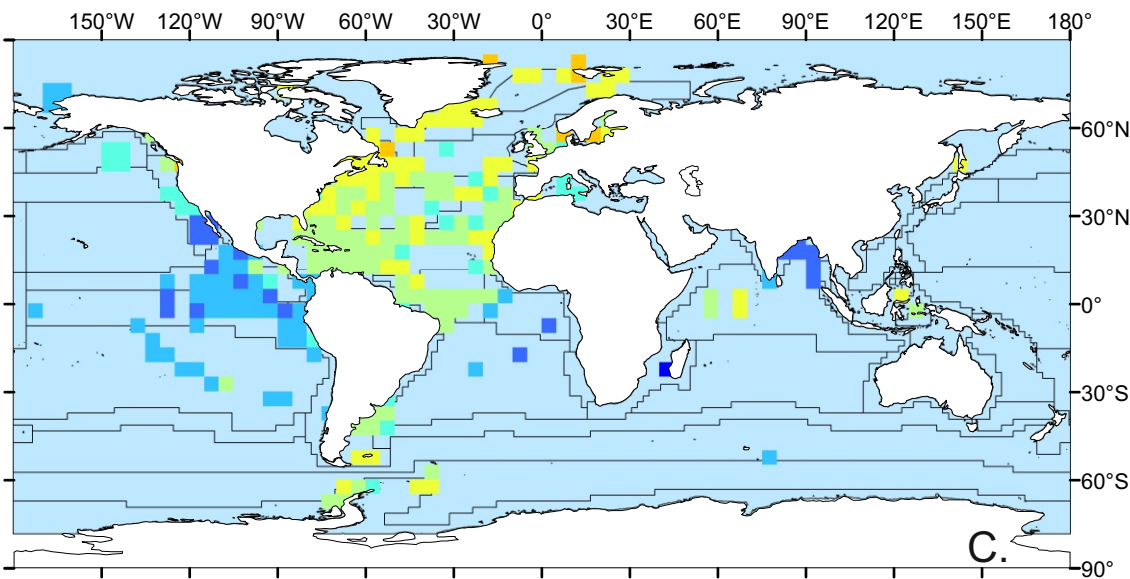
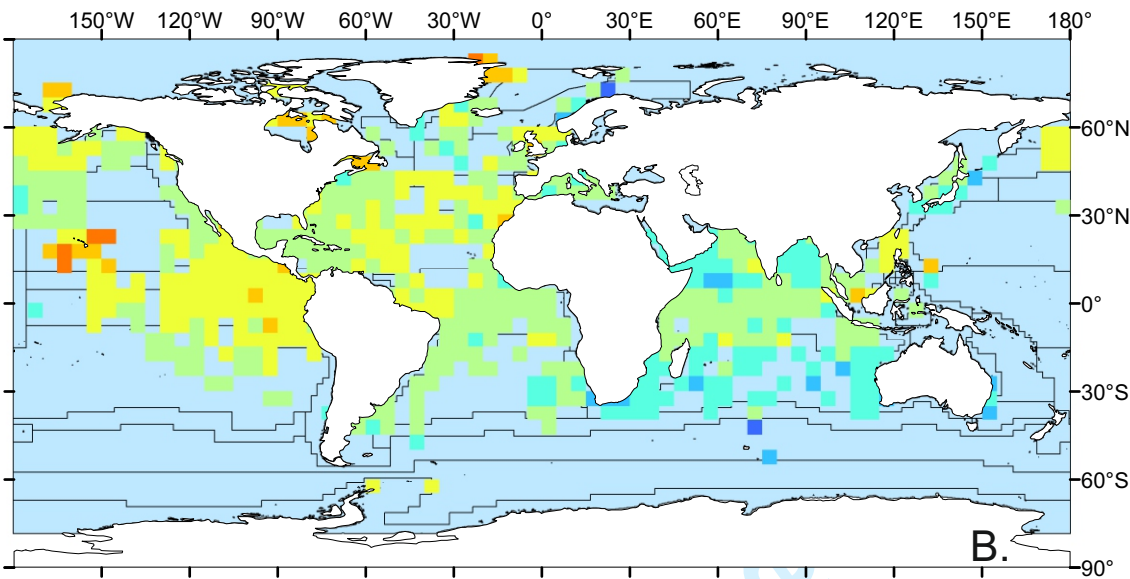
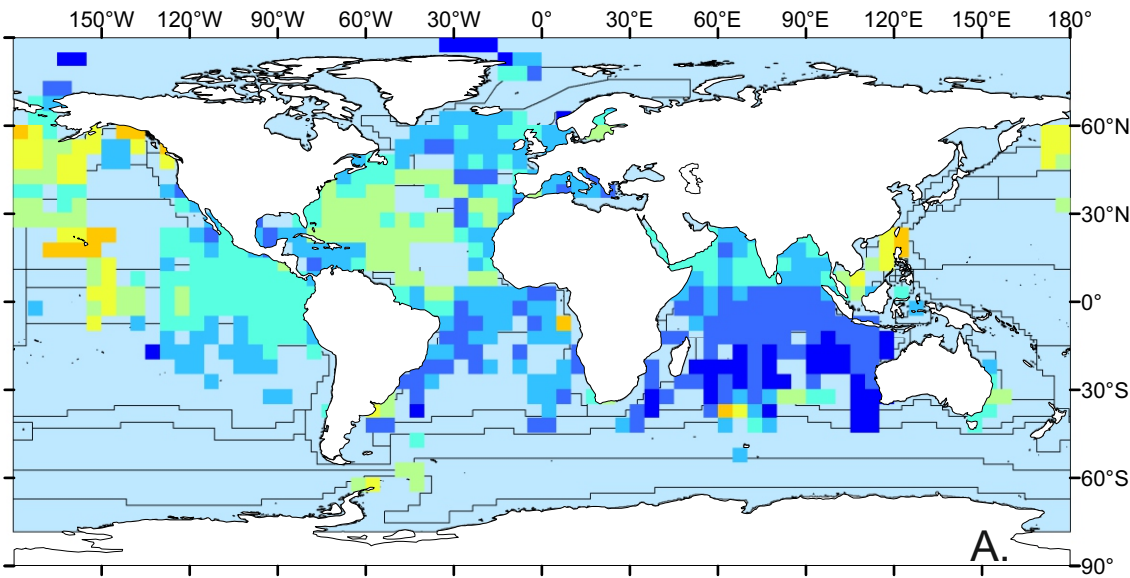
ordinary residual for the i -th observation, x_{ik} is the i -th observation of the k -th predictor and b_k is the regression coefficient estimate for the k -th predictor. Regression lines indicate partial fits.

For Peer Review

1
2
3
4
5
6
7
8
9
10
11
12
13
14
15
16
17
18
19
20
21
22
23
24
25
26
27
28
29
30
31
32
33
34
35
36
37
38
39
40
41
42
43
44
45
46
47
48
49
50
51
52
53
54
55
56
57
58
59
60

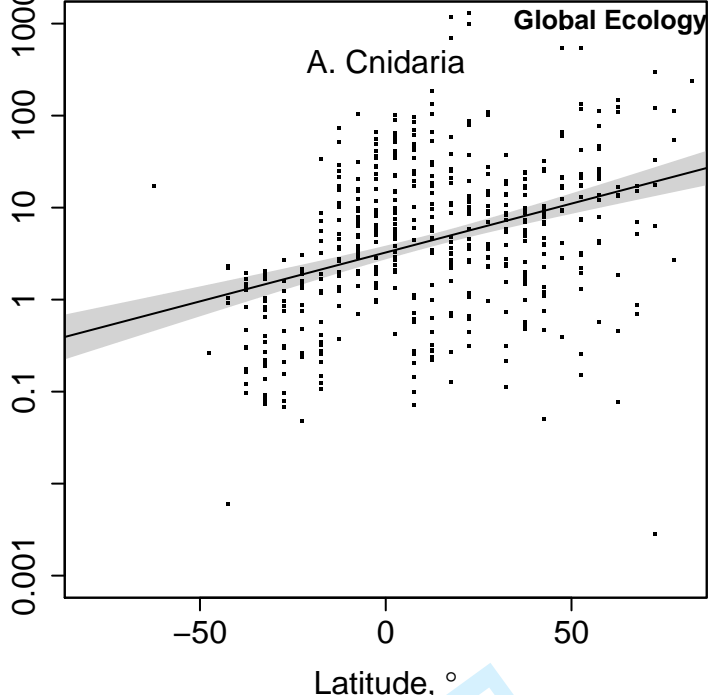


1
2
3
4
5
6
7
8
9
10
11
12
13
14
15
16
17
18
19
20
21
22
23
24
25
26
27
28
29
30
31
32
33
34
35
36
37
38
39
40
41
42
43
44
45
46
47
48
49
50
51
52
53
54
55
56
57
58
59
60

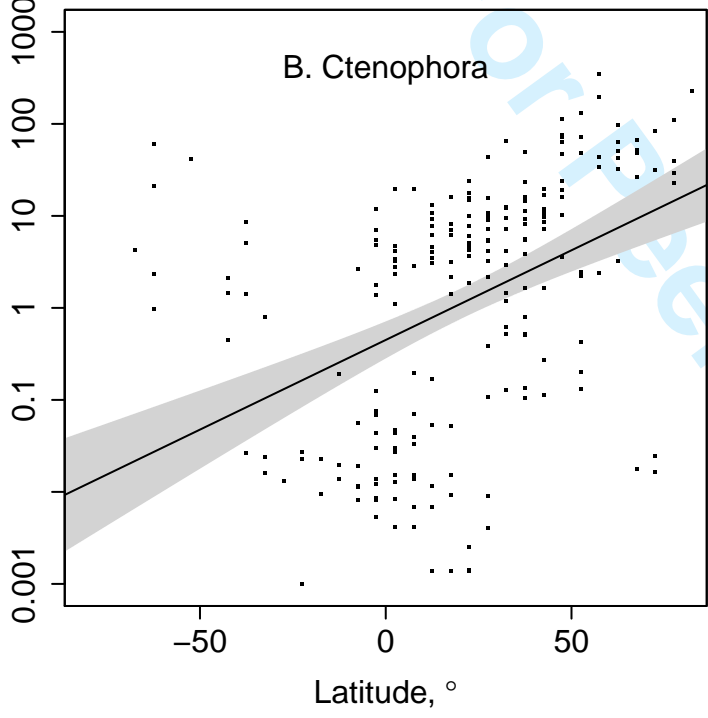


1
2
3
4
5
6
7
8
9
10
11
12
13
14
15
16
17
18
19
20
21
22
23
24
25
26
27
28
29
30
31
32
33
34
35
36
37
38
39
40
41
42
43
44
45
46
47
48
49
50
51
52
53
54
55
56
57
58
59
60

A. Cnidaria



B. Ctenophora



C. Thaliacea

